

# Journal Pre-proof

The role of electrochemical properties of biochar to promote methane production in anaerobic digestion

Ziyan Sun, Lu Feng, Yeqing Li, Yongming Han, Hongjun Zhou, Junting Pan



PII: S0959-6526(22)01900-X

DOI: <https://doi.org/10.1016/j.jclepro.2022.132296>

Reference: JCLP 132296

To appear in: *Journal of Cleaner Production*

Received Date: 14 March 2022

Revised Date: 12 April 2022

Accepted Date: 17 May 2022

Please cite this article as: Sun Z, Feng L, Li Y, Han Y, Zhou H, Pan J, The role of electrochemical properties of biochar to promote methane production in anaerobic digestion, *Journal of Cleaner Production* (2022), doi: <https://doi.org/10.1016/j.jclepro.2022.132296>.

This is a PDF file of an article that has undergone enhancements after acceptance, such as the addition of a cover page and metadata, and formatting for readability, but it is not yet the definitive version of record. This version will undergo additional copyediting, typesetting and review before it is published in its final form, but we are providing this version to give early visibility of the article. Please note that, during the production process, errors may be discovered which could affect the content, and all legal disclaimers that apply to the journal pertain.

© 2022 Published by Elsevier Ltd.

## **CRedit roles**

Ziyan Sun: Experiment, Data curation, Methodology, Resources, Software, Writing - original draft.

Lu Feng: Supervision, Writing – review & editing.

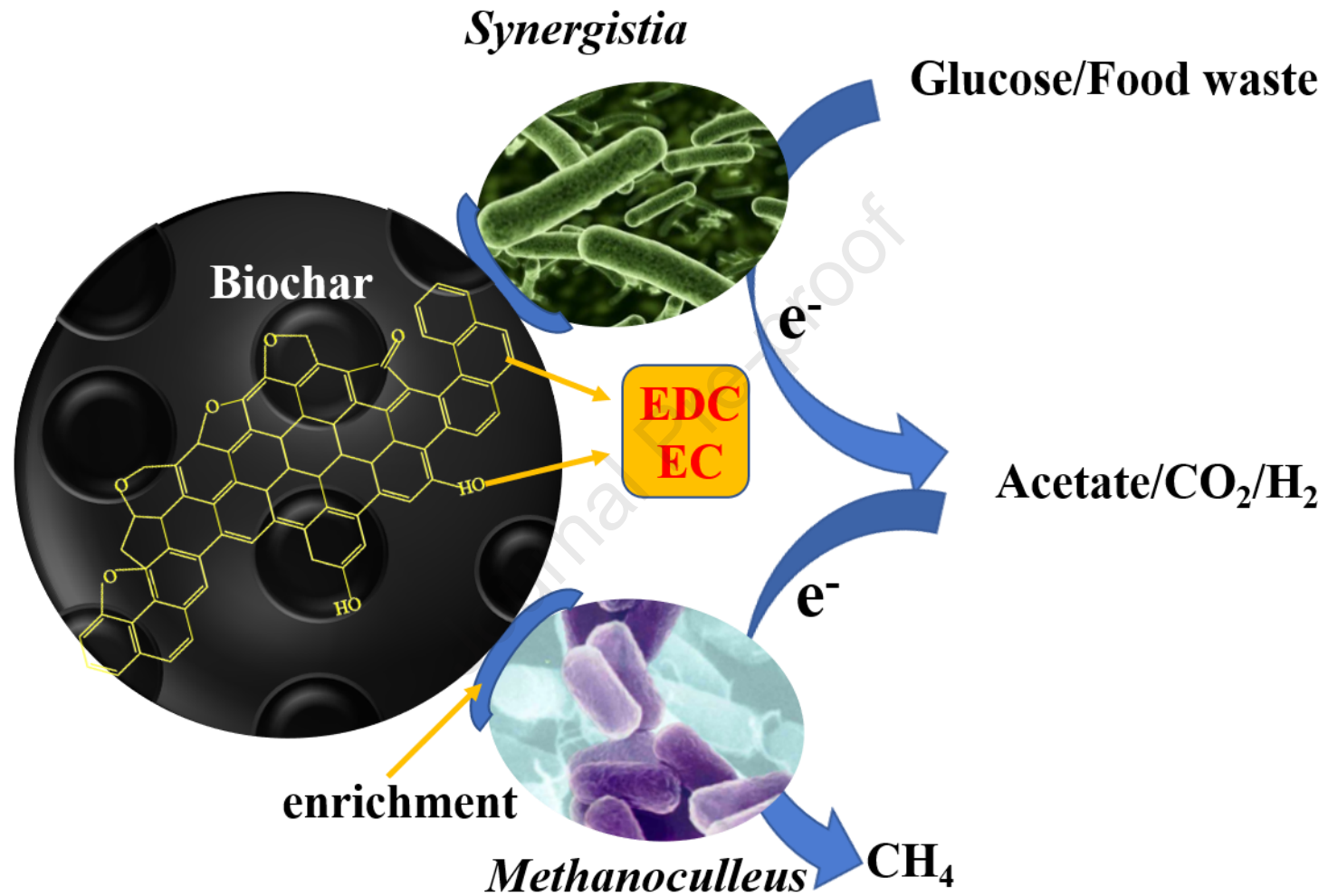
Yeqing Li: Funding acquisition, Investigation, Methodology, Software, Writing - original draft

Yongming Han: Supervision, Writing – review & editing.

Hongjun Zhou: Supervision, Writing – review & editing.

Junting Pan: Supervision, Writing – review & editing.

Graphical abstract:



Journal Pre-proof

# The role of electrochemical properties of biochar to promote methane production in anaerobic digestion

Ziyan Sun <sup>a</sup>, Lu Feng <sup>b</sup>, Yeqing Li <sup>a, \*</sup>, Yongming Han<sup>c</sup>, Hongjun Zhou <sup>a</sup>, Junting Pan <sup>d, \*</sup>

- a. State Key Laboratory of Heavy Oil Processing, Beijing Key Laboratory of Biogas Upgrading Utilization, College of New Energy and Materials, China University of Petroleum Beijing (CUPB), Beijing 102249, PR China;
- b. NIBIO, Norwegian Institute of Bioeconomy Research, P.O. Box 115, N-1431 Ås, Norway;
- c. College of Information Science & Technology, Beijing University of Chemical Technology, Beijing 100029, China;
- d. Institute of Agricultural Resources and Regional Planning, Chinese Academy of Agricultural Sciences, Beijing 100081, PR China.

## Abstract

The electrochemical properties of biochar may be the key factor to promote anaerobic digestion, which has attracted extensive attention. However, the mechanism and the role of the electrochemical properties of biochar are remaining unclear. In this study, biochar with different electrochemical properties was prepared by pyrolysis at different temperatures (BC300/600/900) and oxidation or reduction modification (O/RBC300/600/900). The biochar was added as an additive to promote methanogenic performance of anaerobic digesters of glucose and food waste anaerobic. In both anaerobic digestion systems, the cumulative methane production of food waste increased by 42.07% and the maximum methane production of glucose enhanced by 17.80% after BC900 treatment. RBC600 was inferior to BC900, but superior to BC600. Microbiological analysis suggests that biochar enriched the relative abundant *Synergistia* and *Methanoculleus*. This is conducive to the establishment of the direct interspecies electrons transfer (DIET). Results from correlation analysis, principal component analysis and machine learning confirmed that both of the electron donating capacities (EDC) and electrical conductivity (EC) are dominated factors affecting the cumulative methane yield. Through the analysis of electrochemical properties and preparation process of biochar, the results showed that the pyrolysis temperature increases and the content of phenolic hydroxyl decreases under moderate temperature of biochar, which was beneficial to the methane production. This study found the key factors of the electrochemical properties of biochar in anaerobic digestion, provided new insights for the mechanism of biochar promoting anaerobic digestion and proposed novel directions for the preparation of biochar.

**Keywords:** Anaerobic digestion; Biochar; Electron donating capacities; Electrical conductivity; Oxidation and reduction modification.

42

Abbreviations	
BC	biochar
OBC	oxidation modified biochar
RBC	reduction modified biochar
DIET	direct interspecies electrons transfer
CMs	conductive materials
OCFGs	oxygen-containing functional groups
EDC	electron donating capacities
EC	electrical conductivity
VFAs	volatile fatty acids
EAC	electron accepting capacities
TS	total solid
VS	volatile solid
MEO	mediated electrochemical oxidation
MER	mediated electrochemical reduction
FTIR	fourier to transform infrared spectroscopy
XGBoost	Extreme Gradient Boosting
AI	aromaticity index
DBE	double bond equivalent

43

44

45

46

47

48

49

50

51

52

53

54

55

56

57

58

59

60 

---

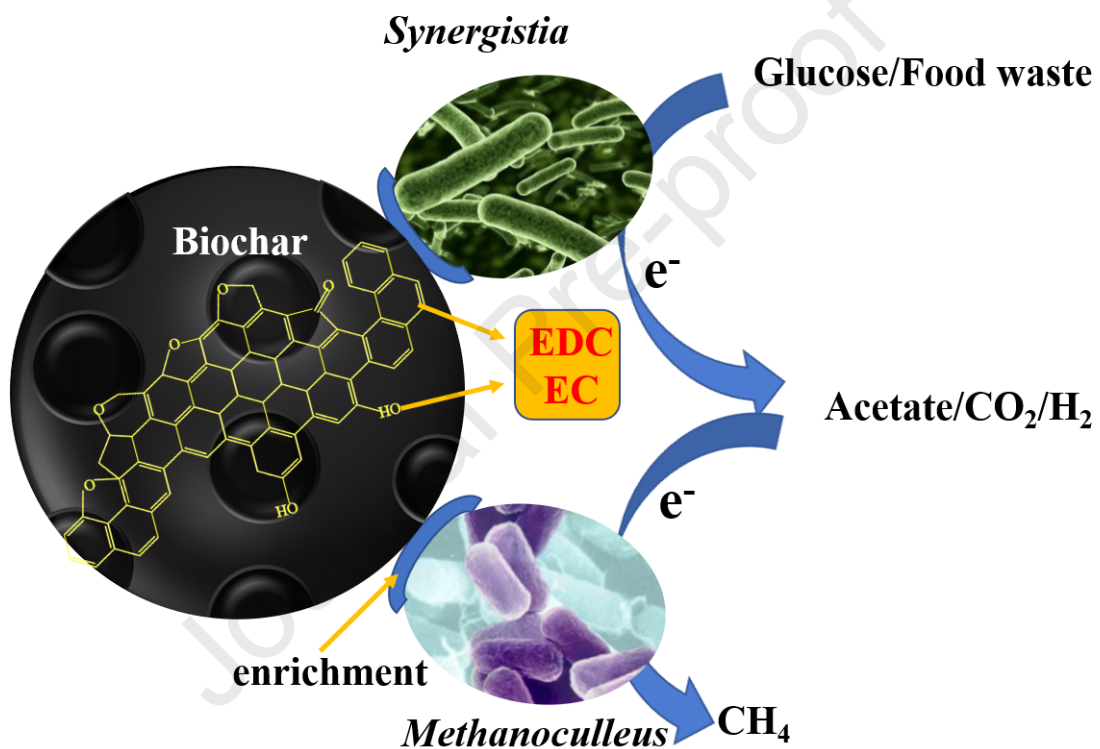
\*Corresponding author.

61 Email address: liyeqingcup@126.com (Prof. Yeqing Li), panjunting@caas.cn (Prof.

62 Junting Pan).

63 **Highlights:**

- 64 • BC900 increased the cumulative methane production of food waste by 42.07%;
- 65 • BC900 increased the maximum methane production rate of glucose by 17.80%;
- 66 • RBC600 was inferior to BC900, but superior to BC600 in anaerobic methanation;
- 67 • Electron donating capacities and electrical conductivity of biochar are keys factors;
- 68 • Higher pyrolysis temperature and lower phenolic hydroxyl of biochar are beneficial.

69 **Graphical abstract:**

70

71

72

73

74

75

76

77

78

79

80

81

## 82 1. Introduction

83 Anaerobic digestion is a well-developed method for treating residues as it could  
84 both generate bioenergy as the form of biogas and recovery nutrients as bio-  
85 fertilizer(Satchwell et al., 2018). It consists of four stages, hydrolysis, acidogenesis,  
86 acetogenesis and methanogenesis, while each of which is performed by a unique set of  
87 functional microorganisms(Lv et al., 2010). Methanogens is sensitive to environmental  
88 variation and the activity of methanogens could be inhibited by various factors  
89 including (1) accumulation of volatile fatty acids (VFAs); (2) accumulation of  
90 molecular hydrogen; and (3) accumulation of formate(Gahlot et al., 2020). Recent  
91 studies suggested that some bacteria can transfer electrons directly to methanogenic  
92 archaea, so called DIET methanogens pathway(Rotaru et al., 2014). DIET achieves  
93 rapid transformation from wastes to energy(Cheng and Call, 2016).

94 The efficiency of DIET directly relies on conductivity, while addition of  
95 conductive materials (CMs) can be used as the electronic channel to realize the direct  
96 exchange of electrons(Barua and Dhar, 2017). Among these CMs, biochar has  
97 advantages of low cost, wide range of raw materials, large specific surface area,  
98 abundant surface functional groups(Zhao et al., 2021), which is therefore considered as  
99 the most promising CMs to accelerate DIET and enhance the efficiency of anaerobic  
100 digestion(Zhao et al., 2021 , Khalid et al., 2021).

101 Recent years, implementation of biochar to improve DIET and the mechanism  
102 were widely reported. For instance, Quintana-Najer (Quintana-Najera et al., 2021)  
103 reported that the most critical characteristics for biochar to improve the anaerobic  
104 digestion performance is surface oxygen functionality. Results from Qi (Qi et al., 2021)  
105 showed that biochar with more aromatic groups and condensed carbon structure is more  
106 favorable to DIET, while the specific surface area and EDC were found to be the key  
107 properties that biochar could enhance anaerobic digestion by Qin (Qin et al., 2020).  
108 However, the role of electrochemical properties of biochar on anaerobic digestion is yet  
109 fully recognized and the understanding on the impact of electrochemical properties  
110 limited. Moreover, it has been well-recognized that the electrochemical performance of  
111 biochar is also affected by the preparation conditions of biochar. However, there is a  
112 lack of in-depth research to reveal these internal links. The electrochemical properties  
113 of biochar mainly include: pseudocapacitance, EC and capacitance(Chacón et al., 2017).  
114 Pseudocapacitance of biochar is mainly related to the oxidation and reduction capacity  
115 of oxygen-containing functional groups (OCFG<sub>s</sub>) (Chacón et al., 2017 , Klupfel et  
116 al., 2014). The EC of biochar depends greatly on the degree of carbonization(Gabhi et  
117 al., 2017). Capacitance is an ability to store energy electrostatically in the way of  
118 electric charges  
119 (Chacón et al., 2017). Based on our best knowledge, there is very limited study reported  
120 the internal relationship between electrochemical properties and preparation process of  
121 biochar to explore the mechanism of biochar acting on anaerobic system. In addition,  
122 most of the current studies focused on using single substrate or co-substrate for



123 anaerobic digestion. Because of different substrate, anaerobic digestion performance is  
 124 different(Xu et al., 2020). This may hinder the understanding of the role and mechanism  
 125 of biochar addition in anaerobic digestion. Implementation of simple substrates may  
 126 help to understand the mechanism, but complex substrates are closer to reality.

127 In this study, biochar with different electrochemical properties was prepared by  
 128 changing pyrolysis temperatures or processed by oxidation/reduction modification.  
 129 Both the most common simple and complicated substrate (e. g. glucose and food waste)  
 130 were used as to research the mechanism of biochar on promotion of the anaerobic  
 131 digestion process. Therefore, the purposes of this study were as follows: (1) compare  
 132 the effects of biochar on promoting methane production of different anaerobic  
 133 substrates; (2) explore the mechanism of biochar electrochemical properties promoting  
 134 methane production; and (3) reveal the internal relationship between the preparation  
 135 process, electrochemical properties of biochar and promoting methanogenesis.

## 136 2. Materials and methods

### 137 2.1 Materials

138 Dried corn straws collected from Beijing were used for biochar preparation. The  
 139 corn straws were firstly grinded to 20 mesh and stored in sealed bag. Food waste was  
 140 taken from the canteen of China University of Petroleum (Beijing), which was firstly  
 141 removed the large particles, for instance bones, and impurities, following homogeneous  
 142 protocols including grinding and sufficient mixing. Inoculum was collected from stably  
 143 operated biogas plant treating mainly food waste. Total solids (TS) and volatile solids  
 144 (VS) were determined following the APHA (2005). Main characteristics of corn straws,  
 145 food waste and inoculum are shown in Table 1.

146 Table 1 Characteristics of corn straws, food waste and inoculum.

Substrate	TS (%)	VS (%)	C (%)	H (%)	O (%)	N (%)
Corn straws	91.26±3.16	82.59±0.91	49.14	6.62	36.93	0.51
Food waste	27.18±0.22	25.50±0.30	55.47	7.24	33.80	1.80
Inoculum	2.52±0.01	1.02±0.03	-	-	-	-

### 147 2.2 Biochar preparation and modification

148 Biochar is prepared in a tubular furnace. 10g corn straws powder was put into  
 149 tubular furnace within nitrogen atmosphere and heated to 300, 600 and 900 °C, named  
 150 BC300, BC600, and BC900, respectively. The temperature was maintained at the target  
 151 temperature for 1 hour. The obtained biochar was filtered and washed with deionized  
 152 water and ethanol. The cleaned biochar was dried at 80 °C for 12 hours, grounded to 80  
 153 mesh, and kept in a centrifugal tube for sealing preservation.

154 Oxidation: 10 g biochar from the first step with 10mL hydrogen peroxide (H<sub>2</sub>O<sub>2</sub>,  
 155 30%w/w) stirred at 120 rpm for 10 hours. The biochar was then cleaned with deionized  
 156 water. The cleaned biochar was dried at 80 °C for 12 hours, namely OBC 300, OBC600,  
 157 and OBC900, respectively, and stored in a sealed centrifugal tube.

158 Reduction: 10g biochar from the first step was placed in 250mL 2mol/ L sodium  
 159 hydroxide (NaOH) solution, stirred at 120 rpm and 10 hours. The biochar was cleaned

160 with deionized water. The cleaned biochar was placed in an oven, dried at 80 °C for 12  
161 hours, namely RBC300, RBC600 and RBC900, and stored in a sealed centrifugal tube.

### 162 2.3 Anaerobic digestion experiment

163 Glucose and food waste were used as substrates. Batch assay was conducted using  
164 both 10gVS/L of substrates and inoculum, with addition of 10g/L of biochar. The  
165 incubation temperature was 37 °C, the rotation speed was 80rpm. Nitrogen was flushed  
166 into the system for 3-5 minutes to create anaerobic condition. Each group was carried  
167 out duplicate. Methane production was recorded by Automatic Methane Potential Test  
168 System II (AMPTSII) (Bioprocess Control, Sweden). Preparation of biochar and  
169 experiment set-up are shown in Fig.1(a).

### 170 2.4 Analysis methods of biochar

171 Biochar yield is determined by the mass percentage of biochar to the raw material.  
172 The moisture, ash content, volatile matter and fixed carbon of biochar were determined  
173 according to GBT212-2008 coal industrial analysis method. The element content of  
174 biochar was performed by elemental analyzer (EA3000, EuroVector, Italy), and the O  
175 content was calculated by difference. The EDC and electron accepting capacities (EAC)  
176 of biochar were quantitatively determined by means of mediated electrochemical  
177 oxidation (MEO)/reduction (MER) method. The details regarding the specific methods  
178 are reported by Klupfel(Klupfel et al., 2014). The OCFGs of obtained biochar were  
179 quantitatively analyzed by Boehm titration method. The detailed methods were  
180 described in the method S1. Other physical and chemical properties of biochar and  
181 microbial community analysis methods refer to previous studies of our research  
182 group(Li et al., 2022b).

### 183 2.5 Data processing and analysis

184 The modified Gompertz model is used to describe the gas dynamic characteristics  
185 of each treatment, as shown in Equation (1):

$$186 \quad P = P_0 \times \exp \left\{ -\exp \left[ \frac{R \times e}{P_0} \times (\lambda - t) + 1 \right] \right\} \quad (1)$$

187 Among them,  $t$  is fermentation time (d),  $P$  represents the cumulative methane  
188 production (mLCH<sub>4</sub>/g VS),  $P_0$  is the methane production potential (mLCH<sub>4</sub>/g VS),  $R$  is  
189 the maximum methane production rate (mLCH<sub>4</sub>/g VS·d), and  $\lambda$  is the lag period (d).

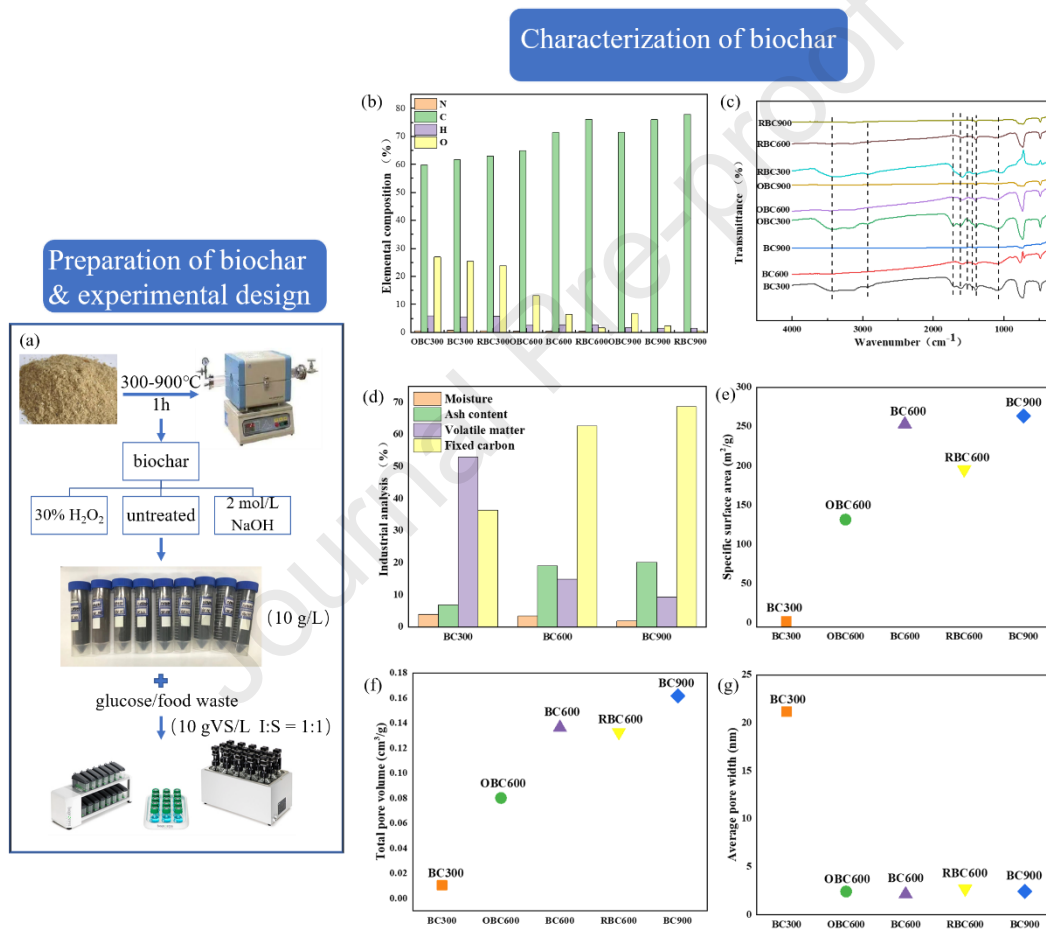
190 Microsoft Office Excel (2019) and Origin Pro 2018 (Origin Lab, MA 01060,  
191 U.S.A) were used for graphing and data treatment. IBM SPSS Statistics 21 (IBM, NY  
192 10504, U.S.A) was used to ANOVA on the significance of results, when  $p < 0.05$  was  
193 considered to be statistically significant.

## 194 3. Results and discussion

### 195 3.1 Physicochemical properties of biochar

196 As shown in Fig.S1, the surface becomes rough and the pore wall becomes thinner  
197 of biochar with the increase of pyrolysis temperature. After oxidation or reduction  
198 modification, the pore surface becomes smooth and the disorder degree decreases. In

199 terms of the elemental composition, biochar treated with higher pyrolysis temperature  
 200 had lower nitrogen, hydrogen, and oxygen contents (no nitrogen was detected at 900°C)  
 201 in Fig.1(b). However, there is a opposite trend observed for carbon, which could be  
 202 explained as the dehydration and decarboxylation reaction occurs at higher temperature  
 203 and that reduces functional groups(Qi et al., 2021). Moreover, modification of biochar  
 204 has limited impact on the nitrogen and hydrogen content but has huge impact on the  
 205 content of carbon and oxygen. Carbon from oxidation modified biochar decreased  
 206 dramatically, accompanying with significantly higher oxygen content. Biochar treated  
 207 with reduction process, however, presented oppositely. These results indicated that  
 208 OCFGs were successfully introduced to the surface of biochar modified by H<sub>2</sub>O<sub>2</sub>, while  
 209 the reducibility of biochar modified by NaOH increased.



210 Fig.1. Schematic diagram of the experimental set-up and characterization of biochar:  
 211 (a) preparation of biochar and the experiment design, (b-g) characterization results of  
 212 biochar.

213 The functional groups of biochar can be determined by FTIR (Fig. 1(c)). The  
 214 absorption peaks at 3600-3200cm<sup>-1</sup> are caused by vibration of hydroxyl groups of  
 215 polymers, such as alcohol, phenol and carboxylic acids; the characteristic peaks of  
 216 2900-2800cm<sup>-1</sup> indicate the presence of aliphatic C-H; the absorption peak at 1700cm<sup>-1</sup>  
 217 is caused by C=O stretching vibration of carbonyl, quinone, ester and carboxyl group;

218 the absorption peaks of  $1650\text{-}1450\text{cm}^{-1}$  are caused by stretching vibrations of C=C  
219 bonds in aromatic or benzene ring structures; the absorption peak at  $1650\text{ cm}^{-1}$  indicates  
220 the presence of C=O (Bhushan et al., 2020 , Wang et al., 2018). The FTIR spectra shown  
221 that the characteristic peaks decreased as the increased pyrolysis temperature. It  
222 indicates that decarboxylation and carbonylation reactions occurred during high  
223 temperature pyrolysis, while most OCFGs were removed. OCFGs were found more  
224 abundant as only cellulose was pyrolyzed but not lignin at  $300\text{ }^{\circ}\text{C}$  (Zhang et al., 2019b).  
225 Lignin started to be pyrolyzed when the temperature rising to  $600\text{ }^{\circ}\text{C}$ , resulting the large  
226 loss of OCFGs. C-O-C bond was also observed, which is probably sourced from the  
227 un-pyrolyzed lignin. There is almost no characteristic peak observed at  $900^{\circ}\text{C}$ ,  
228 indicating that biochar has been graphitized at that temperature (Wan et al., 2019).

229 As shown in Fig.(d), both the moisture and volatile content decreased as a result  
230 of increased pyrolysis temperature, while ash content and fixed carbon content  
231 increased. The results showed that the components of straw were decomposed and  
232 gradually converted from aliphatic carbon to aromatic carbon with the increase of  
233 pyrolysis temperature. During the pyrolysis process, lignocellulosic biomass is first  
234 depolymerize into oligosaccharides, and then generated to biochar, bio-oil, and  
235 pyrolysis gas through dehydration, decarboxylation, aromatization, intramolecular  
236 condensation, and other reactions(Kambo and Dutta, 2015). The ash consists of mainly  
237 silicon, alkali metal, and alkali earth metal element, while the pyrolysis process has  
238 very limited impact on the absolute content(Li et al., 2017b). Organic matter such as C,  
239 H and O is decomposed, and minerals are accumulated at the end of pyrolysis(Enders  
240 et al., 2012). Fixed carbon content represents the carbon sequestration capacity of  
241 biochar itself. Fixed carbon content was significantly increased from 36.39 to 62.70%  
242 as the pyrolysis temperature increased from 300 to  $600\text{ }^{\circ}\text{C}$ . However, the fixed carbon  
243 content didn't change significantly with pyrolysis temperature up to  $900\text{ }^{\circ}\text{C}$ , indicating  
244 that the biochar was stabilized as most of the organic substances have been  
245 converted(Yang et al., 2020).

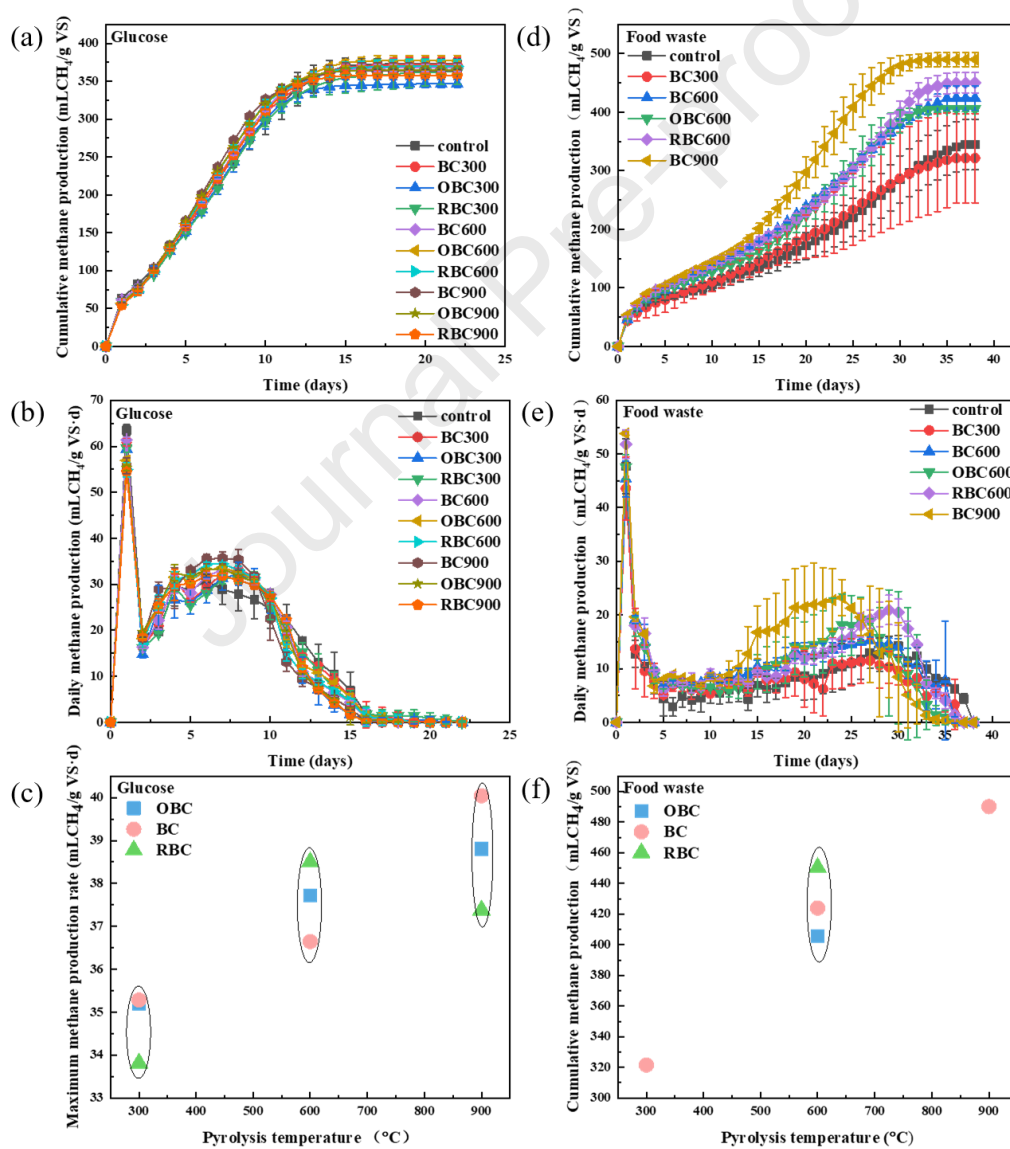
246 The specific surface area characteristics of biochar are considered to be a key  
247 factor that may affect the efficiency of anaerobic digestion as the high specific surface  
248 area and porous structure can promote the loading and immobilization of  
249 microorganisms(Jaafar et al., 2015). The higher the pyrolysis temperature of biochar,  
250 the higher the specific surface area. After oxidation and reduction modification, the  
251 specific surface area of biochar decreased slightly in Fig.(e). The specific surface area  
252 of BC300 is  $1.99\text{ (m}^2\text{/g)}$ , that is significantly lower comparing to BC600 ( $252.97\text{ m}^2\text{/g}$ )  
253 and BC900 ( $263.24\text{ m}^2\text{/g}$ ). This may be explained by the larger amount of not pyrolysis  
254 straw existed in BC300. Based on the results of previous tests, the specific surface area  
255 of raw straw was significantly lower than that of biochar(Qu et al., 2021). Pyrolysis  
256 temperature was found positively affected the pore volume, while modification of  
257 biochar via reduction decreased the pore volume while oxidation had only limited  
258 impact on that in Fig.(f). The pore size of biochar is about 2 nm, with the only exception

259 of BC 300 in Fig.(g). Both oxidation and reduction modification enlarged the pore size  
 260 of biochar, which could be conducive to microbial attachment.

261 3.2 Effect of biochar addition on anaerobic digestion of different substrates

262 3.2.1 Anaerobic digestion of glucose- as simple substrate

263 Different substrates have different degradability and the addition of biochar may  
 264 also have different effects on anaerobic digestion(Xu et al., 2020). At present, most  
 265 studies use a substrate, but the research on the influence of substrate is not enough.  
 266 Therefore, it is necessary to research the influence of biochar on anaerobic digestion of  
 267 different substrate types. In this study, both glucoses (as simple substrate) and food  
 268 waste (as complex substrate) were utilized to better explain the role and mechanism of  
 269 biochar addition on anaerobic digestion.



270 Fig.2. Cumulative methane production, daily methane and effect of pyrolysis  
 271 temperature and modification of biochar on gas production performance:(a-c) glucose



272 as a substrate; (d-f) food waste as a substrate.

273 There was no significant difference between the experimental group with biochar  
 274 addition and the control group without biochar addition except OBC300 ( $p=0.01$ ) and  
 275 RBC900 ( $p=0.029$ ) groups in Fig 2 (a). The control group achieves up to 99.8% of  
 276 theoretical methane production (373.4 mLCH<sub>4</sub>/g VS). Glucose, the most common  
 277 simple substrate, is almost completely degraded. During anaerobic digestion, glucose  
 278 could be directly used to produce methane and there no inhibitory intermediates such  
 279 as ammonia is released. Therefore, the addition of biochar has very limited effect on  
 280 promoting of methane production. This is in accordance with Ren and Li. Ren(Ren et  
 281 al., 2020) added four types of hydrochar to glucose anaerobic digestion system but  
 282 failed on promoting methane production. Li(Li et al., 2022b) added biochar and  
 283 hydrochar to ethanol anaerobic digestion system, respectively. The results also failed to  
 284 increase cumulative methane production.

285 According to Fig. 2 (b) and Table 2, although the addition of biochar failed to  
 286 promote the cumulative methane production from glucose, it promoted the methane  
 287 production rate (RBC 300 is the only exception). The addition of BC900 achieves the  
 288 highest methane production rate, which is 17.80% higher than control. The maximum  
 289 methane production rate of RBC600 was 5.47% higher than BC600 and 13.27% higher  
 290 than control group. As shown in Fig. 2 (c), the increase of pyrolysis temperature and  
 291 reduction modification at medium temperature of biochar both have beneficial effects  
 292 for the methane production rate. However, addition of biochar has no impact on shorten  
 293 the lag time.

294 Table 2 The modified Gompertz model anaerobic digestion with glucose as substrate.

Group	P <sub>0</sub> (mLCH <sub>4</sub> /g VS)	R (mLCH <sub>4</sub> /g VS·d)	λ (d)	R <sup>2</sup>
Control	389.06	33.99	0.11	0.993
BC300	386.88	35.28	0.34	0.993
OBC300	359.00	35.20	0.37	0.990
RBC300	375.72	33.81	0.32	0.993
BC600	381.09	36.64	0.40	0.991
OBC600	390.00	37.72	0.47	0.994
RBC600	380.76	38.50	0.57	0.994
BC900	374.44	40.04	0.56	0.993
OBC900	376.49	38.80	0.52	0.993
RBC900	369.83	37.38	0.52	0.992

### 295 3.2.2 Anaerobic digestion of food waste- as complex substrate

296 When food waste as substrate, the cumulative methane production of the control  
 297 group was not significantly different with BC300 ( $p=0.458$ ) and OBC600 ( $p=0.07$ ), but  
 298 was significantly different with BC600 ( $p=0.024$ ), RBC600 ( $p=0.005$ ) and BC900 ( $p=0$ )  
 299 in Fig.2(d). Compared with glucose as substrate, the addition of biochar significantly

300 promoted the cumulative methane production when food waste was used as substrate.  
301 The contents of protein and lipids in food waste are high, and it is easy to produce  
302 inhibitors such as ammonia, hydrogen sulfide and long-chain fatty acids, which reduces  
303 the stability of the system and leads to the decrease of methane production (Xu et al.,  
304 2018). The addition of biochar improves the buffering capacity of the system, reduces  
305 the ammonia concentration, and promotes the stability of the reactor and methane  
306 production (Pan et al., 2019, Giwa et al., 2019). The cumulative methane production  
307 increases with the increase of pyrolysis temperature of biochar and the effect of  
308 reducing modified biochar on promoting methane production was better than that of  
309 unmodified biochar at the medium pyrolysis temperature in Fig. 2 (f). Compared to the  
310 control group, the cumulative methane production of BC900 increased by 42.07%;  
311 BC600 raised by 22.90%; and RBC600 enhanced by 30.55%.

312 Fig.2(e) presents two gas production peaks of each gas curve; first peak appears  
313 on day 1 and the second is observed between day 24-30. In the first peak, the results  
314 were similar between the control and the experimental groups. The experimental group  
315 with biochar added reached the second peak gas production earlier than the control  
316 group. Except BC300, the peak of gas production of biochar group was higher than  
317 control group. Biochar also has a positive effect for the methane production rate.

318 In conclusion, the influence of biochar on anaerobic digestion of different  
319 substrates is indeed different. For simple substrates, the addition of biochar can promote  
320 the rate of methane production. For complex substrates, biochar can also increase  
321 cumulative methane production. The increase of pyrolysis temperature and reduction  
322 modification at the middle pyrolysis temperature of biochar are conducive to promoting  
323 cumulative methane production. As we all know, the higher the pyrolysis temperature  
324 of biochar, the lower the yield, and the higher the safety requirements for equipment.  
325 Therefore, biochar modified with reduction could achieve reasonable yield under  
326 moderate temperature and therefore is more feasible.

### 327 3.2.3 Microbial community analysis

328 To research the diversity of microorganisms in the environment, the species  
329 abundance and diversity of environmental microbial community can be understood  
330 through single sample Alpha diversity analysis, including Coverage, Sobs, ACE, Chao,  
331 Shannon and Simpson statistical analysis index, as shown in Table 3. Sobs index  
332 reflects the actual number of observed species in the sample. As shown in Table 3, the  
333 number of species from the experimental group with biochar addition was larger than  
334 that in the control group except for the BC300 in archaea. It showed that the addition  
335 of biochar increased the number of microorganisms. Coverage index represents the  
336 coverage of the sample library, the higher value represents the higher probability of  
337 sequence detection in the sample (Li et al., 2018). The coverage index of 12 samples in  
338 this test was all greater than 0.99, indicating that the detection results can reflect the  
339 real situation of most of the bacteria and archaea in the samples.

340 Ace and Chao1 index reflected microbial community richness, Shannon and

341 Simpson index reflected microbial community diversity(Zhang et al., 2020). Among  
 342 them, Shannon, ACE and Chao 1 index were used as ecological indicators(Li et al.,  
 343 2018). The ecological index values of bacterial sequences were large, indicating that  
 344 the diversity and richness of bacteria were much higher than archaea. The results  
 345 showed higher value of Shannon, Chao1 and Ace index were higher, but the Simpson  
 346 index is lower, which had a positive influence to methane production(Li et al., 2017c).  
 347 In this study, the parameters of the biochar group (except BC300) meet the above rules.

348 Table 3 Alpha diversity of the bacteria and archaea.

	Sample	Coverage	Sobs	Ace	Chao1	Shannon	Simpson
Bacteria	control	0.998	478.00	561.178	573.509	3.775	0.066
	BC300	0.999	529.00	594.659	612.720	3.791	0.067
	OBC600	0.999	529.00	592.953	587.043	3.767	0.081
	BC600	0.998	494.00	563.623	555.119	3.536	0.105
	RBC600	0.998	494.00	594.378	611.283	3.333	0.133
	BC900	0.999	486.00	551.638	552.455	3.641	0.091
Archaea	control	1.000	88.00	105.951	98.059	0.989	0.600
	BC300	1.000	86.00	91.265	87.800	1.287	0.466
	OBC600	1.000	93.00	105.355	100.059	1.380	0.418
	BC600	1.000	98.00	128.544	116.455	1.349	0.445
	RBC600	1.000	101.00	189.561	151.214	1.249	0.490
	BC900	1.000	111.00	148.325	137.714	1.126	0.468

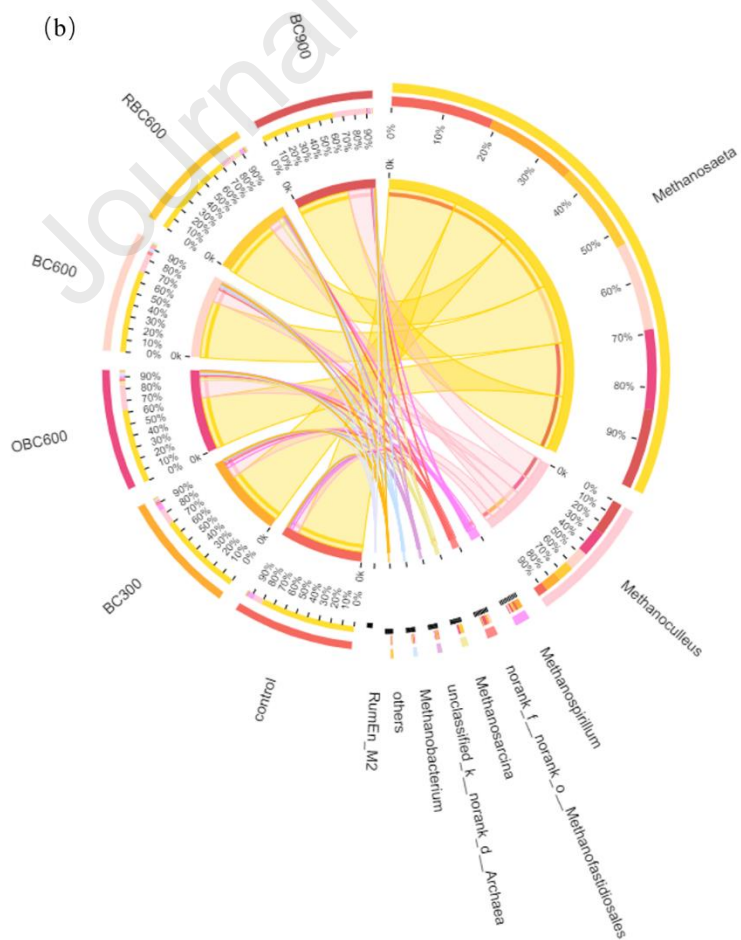
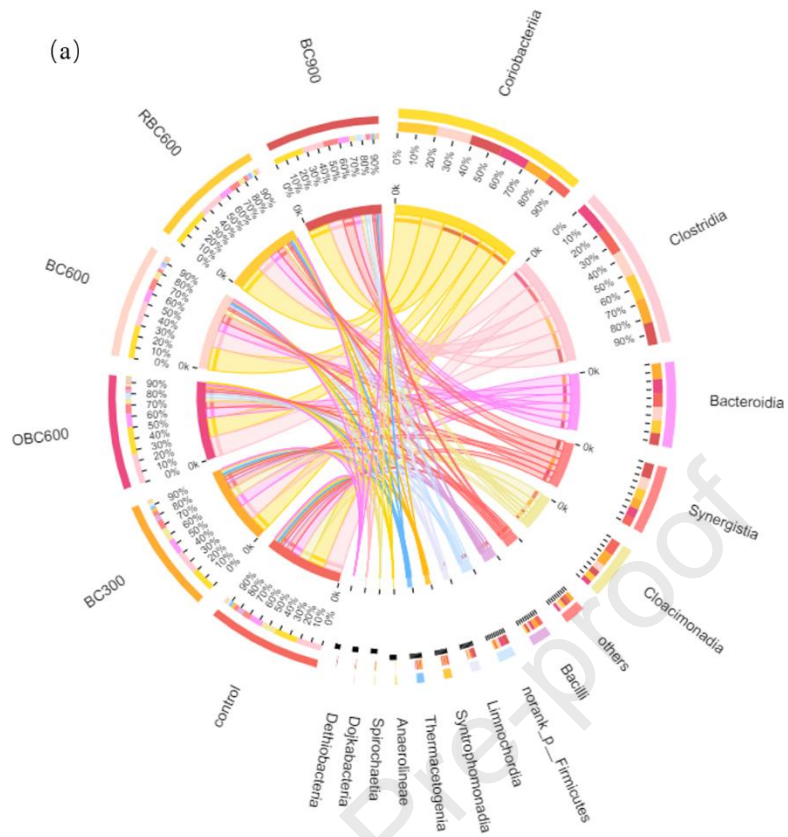
349  
 350 Fig.3 (a) and (b) reflects the distribution proportion of dominant species in each  
 351 sample and the distribution proportion of dominant species in different samples through  
 352 the visual circle diagram. In Fig.3(a), the class level bacterial community is dominated  
 353 by *Coriobacteriia* (13-21%), *Clostridia* (14-17%), *Bacteroidia* (15-19%), *Synergistia*  
 354 (14-23%) and *Cloacimonadia* (9.9-28%). The addition of biochar enhanced the relative  
 355 abundance of *Coriobacteriia* and *Synergistia*, decreased the abundance of  
 356 *Cloacimonadia*, but had little effect on the abundance of *Clostridia* and *Bacteroidia*.  
 357 RBC600 had the highest *Coriobacteriia* (21%). BC900 had the highest *Synergistia*  
 358 (23%). *Coriobacteriia* is associated with the production of formic, lactic and acetic  
 359 acids(Li et al., 2022a). The increase of relative abundance of *Coriobacteriia* indicated  
 360 that the addition of biochar promoted the formation of formic acid, lactic acid and acetic  
 361 acid. The abundance of *Coriobacteriia* of RBC600 was 10.53% higher than BC600,  
 362 indicated that reduction modification of biochar was more conducive to the occurrence  
 363 of this process. Addition of biochar enriched methanogens that can only use  
 364 monocarbon, acetic acid and hydrogen/carbon dioxide as substrates directly(Demirel  
 365 and Scherer, 2008). Biochar effectively enriched *Coriobacteriia*, which has positive  
 366 impact on methane generation. The control group has the most abundant  
 367 *Cloacimonadia*. Some genera in *Cloacimonadia* convert amino acid, sugars or alcohols



368 to VFAs(Ni et al., 2020). The addition of biochar reduced the relative abundance of  
369 *Cloacimonadia*, which possible be related to the enhancement of buffering capacity of  
370 anaerobic system by biochar. *Synergistia* is a typical symbiotic fermentation bacterium,  
371 usually symbiosis with hydrotrophic methanogenic archaea to overcome  
372 thermodynamic energy barrier and promote the degradation and metabolism of VFAs  
373 to generate methane(Świątczak et al., 2017). The addition of biochar effectively  
374 enriched *Synergistia*. The relative abundance of *Synergistia* is 14% (control), 15%  
375 (BC300), 15% (OBC600), 18% (BC600), 16% (RBC600) and 23% (BC900),  
376 respectively, corresponding to an increment of 7.14% (BC300), 7.14 (OBC600), 28.57  
377 (BC600), 14.28% (RBC600) and 64.28% (BC900), respectively.

378 *Methanosaeta* and *Methanoculleus* are main archaeal genus in Fig.3(b).  
379 *Methanosaeta* is an obligate acetic acid nutritive methanogenic archaeon(Vavilin et al.,  
380 2008 , Zhang et al., 2018a). *Methanoculleus* is hydrogenotrophic methanogen. The  
381 relative abundance of *Methanosaeta* was similar in each group. However, the addition  
382 of biochar effectively enriched *Methanoculleus*. The relative abundance of  
383 *Methanoculleus* increased from 8.3% (control) to 13% (BC300), 21% (OBC600), 16%  
384 (BC600), 13% (RBC600) and 28% (BC900), respectively. Addition of BC 900 had the  
385 most abundant *Methanoculleus*, which was 3.37 times that of the control group.  
386 *Methanoculleus* is a typical syntrophic methanogenic Archaea(Wang et al., 2020). The  
387 addition of biochar can effectively enrich *Methanoculleus*, which may be related to the  
388 establishment of DIET(Lim et al., 2020).Because the addition of biochar effectively  
389 enriched *Synergistia* and *Methanoculleus*. Therefore, the addition of biochar may  
390 promote the establishment of DIET between anaerobic fermentation bacteria and  
391 methanogenic archaea.

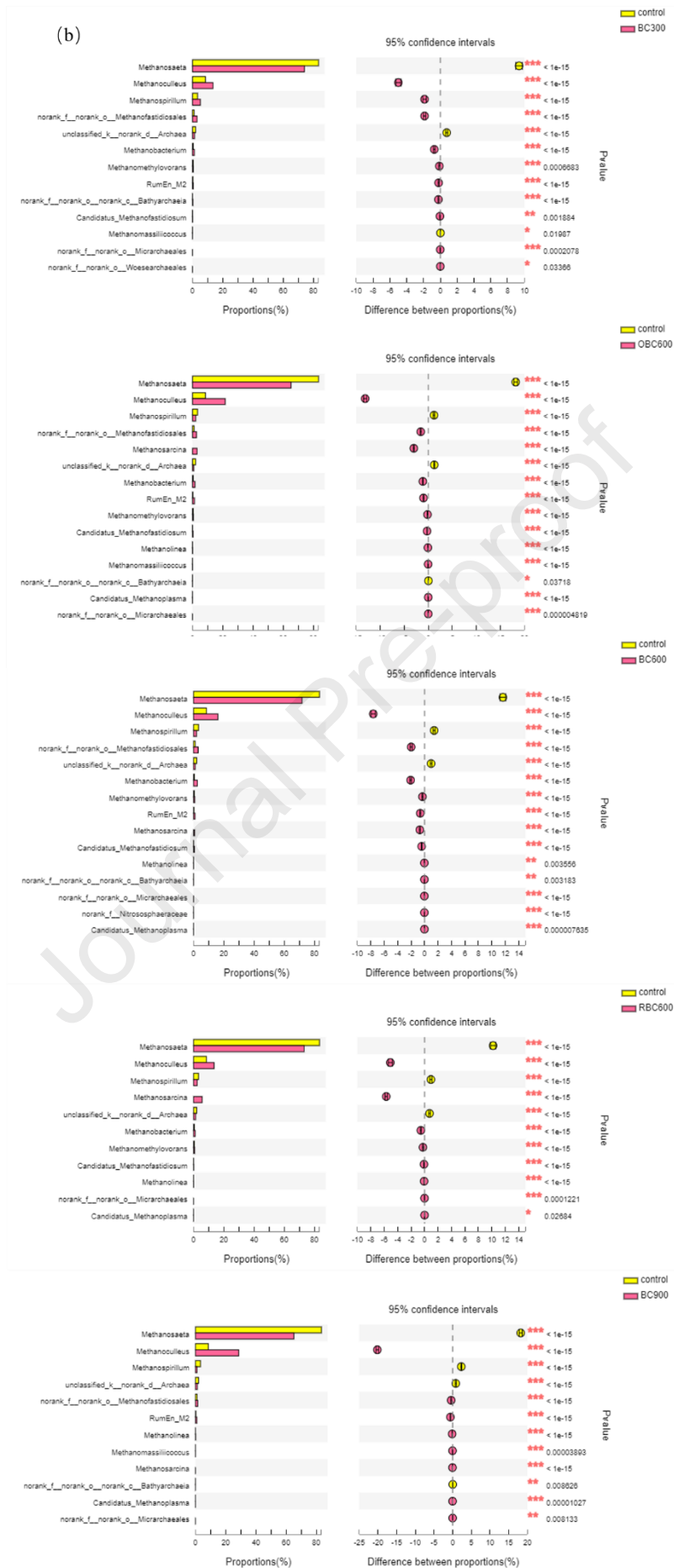
392



394 Fig. 3. Sample and species relationships diagrams of bacteria and archaea: (a) bacteria  
395 at class level; (b) archaea in genus level.

396 According to the abundance data of microbial communities obtained from the test  
397 samples, Fisher' exact test was used to compare the differences of microbial abundance  
398 between two samples. Significant differences of bacteria and archaea between the  
399 control and add biochar group samples were obtained in Fig.4, respectively. Fig.4 (a)  
400 and (b) show the distribution histogram of microorganisms and the abundance  
401 difference between the species in two samples, within 95% confidence interval, as well  
402 as the markers of significance difference (the more marks represent the higher  
403 significance level) and the size of  $p$  value. There is a clear difference observed between  
404 biochar added group and the control, which correlated to the increased pyrolysis  
405 temperature.



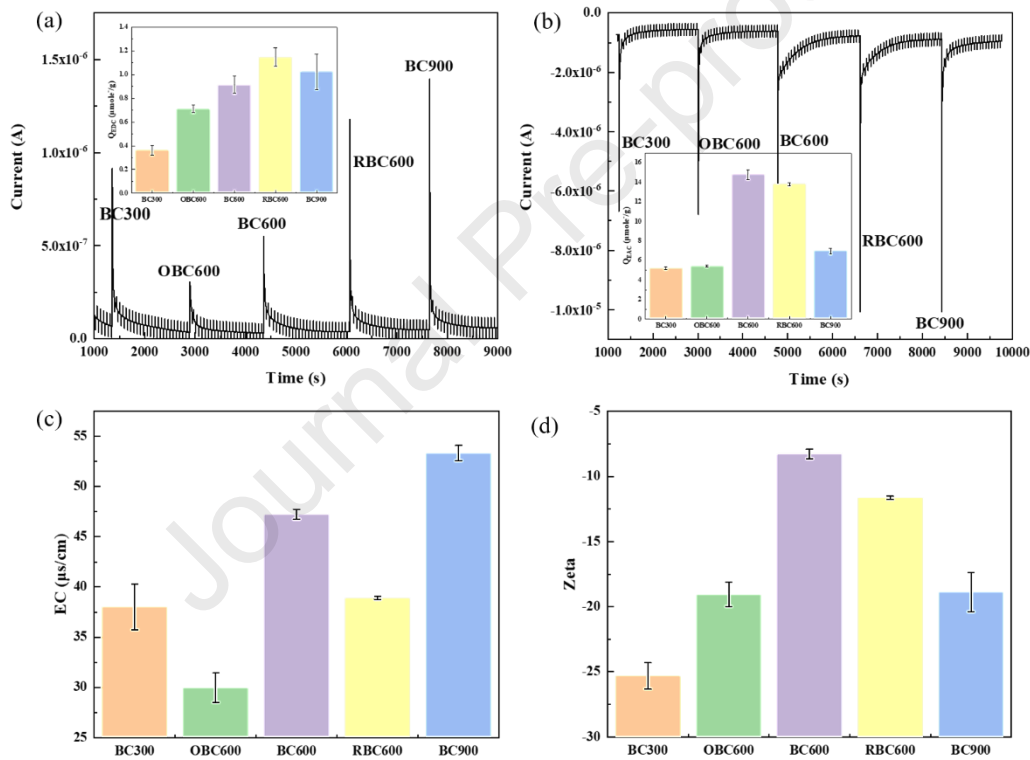


408 (\*:  $0.01 < p \leq 0.05$ ; \*\*:  $0.001 < p \leq 0.01$ ; \*\*\*:  $p \leq 0.001$ )

409 Fig. 4. Analysis diagram of significant difference diagram of bacterial and archaea  
 410 abundance between the control group and add different biochar: (a) bacterial in class  
 411 level; (b) archaea in genus level.

### 412 3.3 Mechanism of biochar electrochemical properties on anaerobic digestion

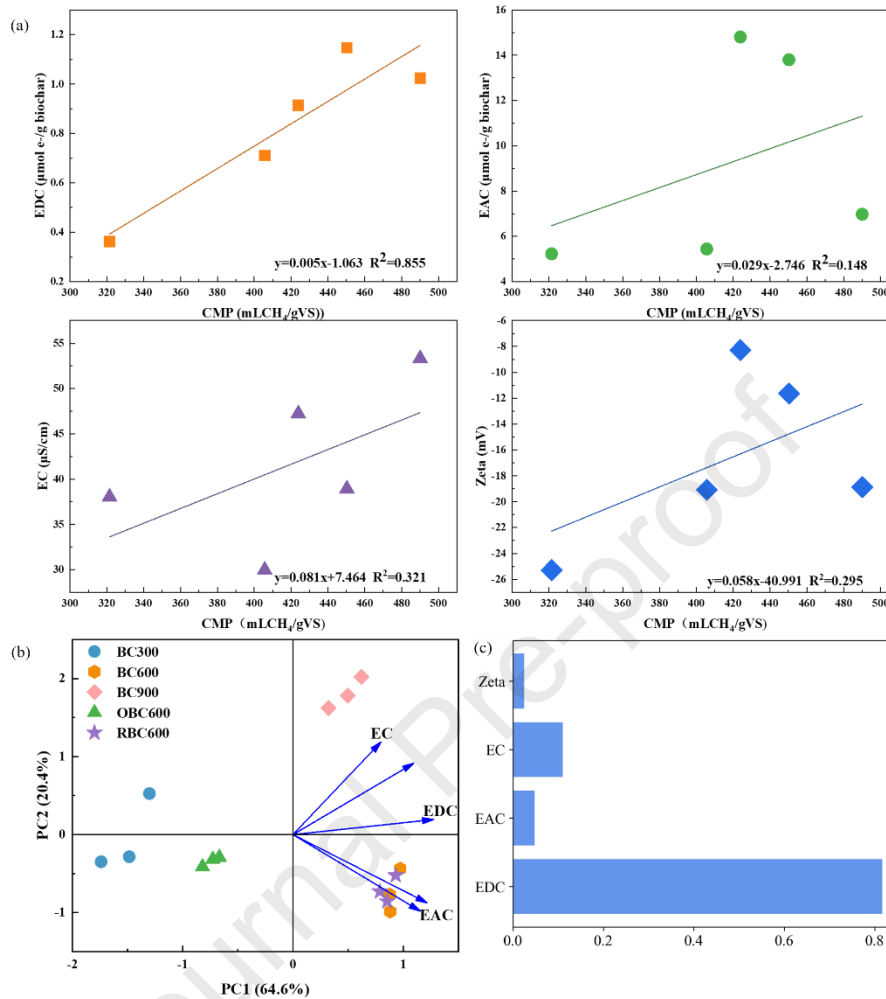
413 The test results of EDC, EAC, EC and Zeta of biochar are shown in Fig.5 (a)-(d).  
 414 The electrochemical properties are affected by oxidation and reduction modification.  
 415 EDC and EAC are mainly related to the ability of gaining and losing electrons of  
 416 OCFGs of biochar(Chacón et al., 2017). Tan (Tan et al., 2020)found that Zeta of biochar  
 417 was also related to OCFGs. However, the conductivity of biochar mainly depends on  
 418 the degree of carbonization(Gabhi et al., 2017). Its relationship with oxygen-containing  
 419 functions has rarely been reported.



420 Fig.5. Electrochemical properties of biochar: (a) EDC; (b) EAC; (c) EC; (d) Zeta.

421 Three analytical methods, linear correlation, principal component analysis and  
 422 machine learning, were accustomed to analyze the relationship between cumulative  
 423 methane production and four electrochemical properties with different mathematical  
 424 perspectives. Linear correlation is the most common analysis of the relationship  
 425 between two variables in anaerobic digestion(Yu et al., 2018 , Liew et al., 2012).  
 426 According to Fig.6 (a), the cumulative methane production is positively correlated with  
 427 EDC, EAC, EC and Zeta potential, while the EDC is the most relevant factor (strongly  
 428 correlated) following with EC (moderately correlated), EAC and Zeta potential (weakly

429 correlated). Principal component analysis is a multivariate statistical method for  
430 dimensionality reduction and is widely accustomed to analyze the interaction between  
431 different factors(Li et al., 2021). Analyses using principal component analysis show  
432 that cumulative methane production has a stronger correlation with EC and EDC (Fig.6  
433 (b)). Extreme Gradient Boosting (XGBoost) in machine learning algorithms has the  
434 advantage of fast learning speed and high prediction accuracy(Xu et al., 2021).  
435 XGBoost shows that EDC and EC are the main feature importance factors affecting  
436 cumulative methane production in Fig.6(c). However, there are different opinions on  
437 the contribution of electrical conductivity to methane production. Ye(Ye et al., 2018)  
438 found that higher conductivity promoted electron transfer between the syntrophic  
439 bacteria and methanogens and promoted methane generation. Baek (Baek et al., 2021)  
440 believes that the conductivity of the material itself does not improve anaerobic digestion  
441 performance. In this study, the conclusion based on three analytical methods revealed  
442 that both EDC and EC are the main factors affecting cumulative methane production.  
443 Multiple regression analysis was performed on them. The fitting equation:  
444  $CMP=171.289[EDC]+1.331[EC]+220.651$  ( $R^2=0.768$ ). The coefficient of EDC is  
445 much larger than that of EC, indicating that EDC is the most dominant factor affecting  
446 the cumulative methane production.



447

448 Fig. 6. The relationship between cumulative methane production and four  
 449 electrochemical properties of biochar: (a) linear correlation; (b) principal component  
 450 analysis; (c) XGBoost feature importance of cumulative methane production.

451

452 3.4 Relationship between electrochemical properties of biochar and its  
 453 preparation process

454

455 Results from 3.3 reflected that the cumulative methane production were mainly  
 456 depended on EDC and EC. According to previous studies, EDC is related to OCFGs  
 457 and carbon structure (Zhang et al., 2018b). Below 650 °C, the EDC of biochar is mainly  
 458 attributed to phenolic hydroxyl groups. Above 650 °C, the conjugated p-electron system  
 459 associated aromatic structure became dominated (Zhang et al., 2018b). EC is related to  
 460 the degree of carbonization. However, in this study, EC is also affected by oxidation  
 461 and reduction modification. Suliman (Suliman et al., 2016) reported irregular  
 462 fluctuations of conductivity with addition of biochar modified with air oxidation.  
 Therefore, it is necessary to deeply research the relationship between the preparation  
 process of biochar and EDC and EC, for purpose of finding the best preparation process



463 of biochar.

464 The OCFGs of biochar were analyzed by XPS and Boehm titration. XPS is used  
 465 to quantitatively characterize the element content and form of materials (XPS results  
 466 are shown in Fig. S2). The C1s spectrum is divided into three peaks: the peak at 284.6-  
 467 284.8eV belongs to aromatic or aliphatic carbon (C-C/C-H); the peak at 285.2-285.8eV  
 468 is the phenolic and alcohol carbon (C-O); the peaks at 287.3-288.2eV are attributed to  
 469 C=O. O1s spectrum is divided into two peaks: the peak at 530.8-531.2eV belongs to  
 470 C=O; The peak at 533.2-533.8eV is attributed to C-O(Singh et al., 2014 , Quintana-  
 471 Najera et al., 2021).

472

Table 4 XPS oxygen and carbon peaks of biochar.

Biochar	C spectrum	O spectrum
Biochar	C-O/C=O	C-O/C=O
BC300	3.29	3.50
OBC600	1.08	1.28
BC600	1.18	1.85
RBC600	0.90	1.13
BC900	0.55	0.73

473 Functional groups containing C-O bonds are mostly reductive groups with electron  
 474 donating capacities, such as phenolic hydroxyl groups. Functional groups containing  
 475 C=O bonds are mostly oxidizing groups with electron accepting capacities, such as  
 476 carbonyl quinone groups. In Table 4, the ratio of C-O/C=O decreases with the raise of  
 477 pyrolysis temperature, while that from RBC600 is lower than BC600 probably due to  
 478 the NaOH neutralizes hydroxyl groups (Zhang et al., 2019a , Li et al., 2017a). The ratio  
 479 from OBC600 was also lower than BC600, which could be explained by the successful  
 480 introduction of C=O functional groups on the surface of biochar (Shen et al., 2019 , Wu  
 481 et al., 2017).

482 Boehm titration was implemented for qualitative and quantitative analysis of  
 483 oxygen-containing functions with different reaction capacities of alkali with different  
 484 strengths and acid OCFGs on the surface of carbon (Fig. S3)(Fidel et al., 2013). It was  
 485 obtained the specific contents of four OCFGs in biochar. The content of OCFGs  
 486 decreases with the raise of pyrolysis temperature. After reduction modification,  
 487 RBC600 contains only phenolic hydroxyl groups which is lower than BC600.

488 Elemental analyzer can quantitate the specific content of each element from  
 489 biochar, while the ratios of different elements could reflect the properties of biochar.  
 490 For example, H/C represents the degree of carbonization and aromatization of biochar;  
 491 lower H/C value indicates high degree of aromatization and carbonization. O/C  
 492 represents the oxidation of biochar while the higher O/C reveals stronger oxidation. It  
 493 is well known that increasing of pyrolysis temperature could enhance the carbonization  
 494 and aromatization of biochar. Koch (Koch and Dittmar, 2006) proposed the general  
 495 aromaticity index (AI) and two thresholds, AI > 0.5 aromatic compounds were found  
 496 in organic matter, and AI  $\geq$  0.67 condensed aromatic compounds were found in organic

497 matter. The higher AI indicates higher the degree of condensation. The unsaturation of  
 498 carbon-carbon double bonds in the molecule should be evaluated before calculating AI.  
 499 The double bond equivalent (DBE) represents the sum of unsaturated rings and double  
 500 bonds in the molecule. DBE and AI are calculated by the Equation (2) and (3),  
 501 respectively:

$$502 \quad DBE = \frac{1 + [C] - 0.5[H] + 0.5[N]}{[C]} \quad (2)$$

$$503 \quad AI = \frac{1 + [C] - [O] - 0.5[H]}{[C] - [O] - [N]} \quad (3)$$

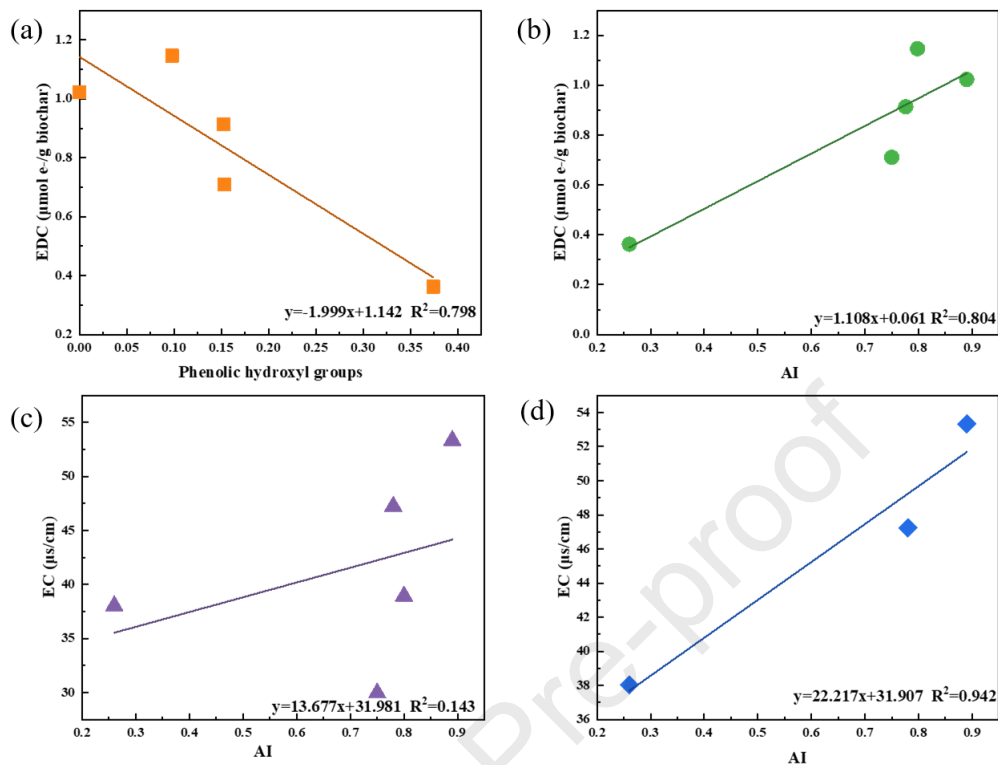
504 As shown in Table 5, the degree of carbonization and aromatic properties are  
 505 increased as a results of higher pyrolysis temperature. AI>0.67 of BC600 indicates  
 506 that condensed aromatic compounds started to appear at with pyrolysis temperature  
 507 above 600°C.

508 Table 5 Ratio of characteristic elements of biochar.

biochar	Mass fraction ratio		molar ratio	
	O/C	H/C	DBE	AI
BC300	0.411	0.089	0.491	0.26
OBC600	0.202	0.039	0.786	0.75
BC600	0.091	0.038	0.792	0.78
RBC600	0.021	0.036	0.800	0.80
BC900	0.030	0.021	0.892	0.89

509  
 510 Correlation analysis between EDC and phenolic hydroxyl groups and AI of  
 511 biochar are shown in Fig.7 (a, b). EDC was found strongly correlated with phenolic  
 512 hydroxyl groups ( $R^2=0.798$ ) and AI ( $R^2=0.804$ ), in which EDC was negatively  
 513 correlated with phenolic hydroxyl groups and positively correlated with AI. Multiple  
 514 regression analysis was performed on EDC and phenolic hydroxyl groups and AI that  
 515 obtained the fitting equation as following:  $EDC = -0.909[Ar-OH] + 0.624[AI] + 0.539$   
 516 ( $R^2=0.630$ ). The coefficients of phenolic hydroxyl and AI were similar, indicating that  
 517 phenolic hydroxyl groups and AI contributed equally to EDC. EC has a good correlation  
 518 with BC300, BC600, and BC900 ( $R^2=0.942$ ) (Fig. 7(d)), which is consistent with most  
 519 conclusions: the conductivity of biochar depends on its carbonization degree (Gabhi et  
 520 al., 2017). However, when OBC600 and RBC600 are added, the correlation becomes  
 521 significantly worse ( $R^2=0.143$ ), indicating that EC is greatly affected by oxidation and  
 522 reduction modification (Fig. 7 (c)).

523



524 Fig. 7. Correlation analysis: (a) EDC and phenolic hydroxyl groups, (b) EDC and AI,  
 525 (c) EC and AI, (d) EC and AI (only BC300, BC600, BC900).

526 In short, the increased pyrolysis temperature improved the carbonization of  
 527 biochar, which further both enhance EDC and EC. After reduction modification, the  
 528 phenolic hydroxyl content of biochar decreased, which had positive impact on EDC but  
 529 unfavorable to EC. Since EC contributes less to methane production, the overall results  
 530 are favorable for promoting anaerobic digestion.

#### 531 4. Conclusions

532 In this study, the influence of biochar with different electrochemical properties on  
 533 the methanogenic performance of anaerobic digesters of different substrates were  
 534 compared. The results indicated that the addition of biochar to simple substrate-glucose  
 535 can promote the methane production rate, while for complex substrate-food waste, the  
 536 cumulative methane production was promoted. In the two anaerobic digestion systems,  
 537 BC900 has the best effect on methanation. The effect of RBC600 is lower than BC900,  
 538 but better than BC600, better than the control group. After BC900 was added, the  
 539 cumulative methane production of food waste and the maximum methane production  
 540 rate of glucose increased by 42.07% and 17.80%, respectively. The addition of biochar  
 541 can effectively enhance the relative abundance of *Synergistia* (7.14-64.28%) and  
 542 *Methanoculleus* (1.57-3.37 times), which is conducive to the establishment of DIET  
 543 system. The ability of biochar to enhance anaerobic digestion largely depends on  
 544 mainly EDC and EC. It was found that EDC and EC could be affected by changing the

545 pyrolysis temperature and OCFGs of biochar. The enhance of pyrolysis temperature or  
546 the decrease of phenolic hydroxyl content under moderate temperature of biochar is  
547 beneficial to methane production. A new direction was pointed out for the preparation  
548 and improving the methanation promoting effect of biochar. The effect of oxidation and  
549 reduction modification on EC and EDC of biochar can be further studied in order to  
550 optimize the preparation process of biochar.

551

552 CRediT authorship contribution statement

553 Ziyan Sun: Experiment, Data curation, Methodology, Resources, Software,  
554 Writing - original draft. Lu Feng: Supervision, Writing – review & editing. Yeqing Li:  
555 Funding acquisition, Investigation, Methodology, Software, Writing - original draft.  
556 Yongming Han: Supervision, Writing – review & editing. Hongjun Zhou: Supervision,  
557 Writing – review & editing. Junting Pan: Supervision, Writing – review & editing.

558

559 Declaration of Competing Interest

560 The authors declare that they have no known competing financial interests or  
561 personal relationships that could have appeared to influence the work reported in this  
562 paper.

563

564 Acknowledgements

565 The study was funded by Science Foundation of China University of Petroleum  
566 Beijing (No.2462020BJRC003; 2462020YXZZ018), the Strategic Cooperation  
567 Technology Projects of CNPC and CUPB (Grant No. ZLZX2020-04).

568

569 References

- 570 Baek G, Rossi R, Saikaly P E, et al. 2021. The impact of different types of high  
571 surface area brush fibers with different electrical conductivity and  
572 biocompatibility on the rates of methane generation in anaerobic digestion. *Sci*  
573 *Total Environ* [J], 787: 147683.
- 574 Barua S, Dhar B R 2017. Advances towards understanding and engineering direct  
575 interspecies electron transfer in anaerobic digestion. *Bioresour Technol* [J], 244:  
576 698-707.
- 577 Bhushan B, Gupta V, Kotnala S 2020. Development of magnetic-biochar nano-  
578 composite: Assessment of its physico-chemical properties. *Materials Today:*  
579 *Proceedings* [J], 26: 3271-3274.
- 580 Chacón F J, Cayuela M L, Roig A, et al. 2017. Understanding, measuring and tuning  
581 the electrochemical properties of biochar for environmental applications.  
582 *Reviews in Environmental Science and Bio/Technology* [J], 16: 695-715.
- 583 Cheng Q, Call D F 2016. Hardwiring microbes via direct interspecies electron  
584 transfer: mechanisms and applications. *Environ Sci Process Impacts* [J], 18: 968-  
585 980.

- 586 Demirel B, Scherer P 2008. The roles of acetotrophic and hydrogenotrophic  
587 methanogens during anaerobic conversion of biomass to methane: a review.  
588 *Reviews in Environmental Science and Bio/Technology [J]*, 7: 173-190.
- 589 Enders A, Hanley K, Whitman T, et al. 2012. Characterization of biochars to evaluate  
590 recalcitrance and agronomic performance. *Bioresour Technol [J]*, 114: 644-653.
- 591 Fidel R B, Laird D A, Thompson M L 2013. Evaluation of modified boehm titration  
592 methods for use with biochars. *J Environ Qual [J]*, 42: 1771-1778.
- 593 Gabhi R S, Kirk D W, Jia C Q 2017. Preliminary investigation of electrical  
594 conductivity of monolithic biochar. *Carbon [J]*, 116: 435-442.
- 595 Gahlot P, Ahmed B, Tiwari S B, et al. 2020. Conductive material engineered direct  
596 interspecies electron transfer (DIET) in anaerobic digestion: Mechanism and  
597 application. *Environmental Technology & Innovation [J]*, 20: 101056.
- 598 Giwa A S, Xu H, Chang F, et al. 2019. Effect of biochar on reactor performance and  
599 methane generation during the anaerobic digestion of food waste treatment at  
600 long-run operations. *Journal of Environmental Chemical Engineering [J]*, 7:  
601 103067.
- 602 Jaafar N M, Clode P L, Abbott L K 2015. Soil Microbial Responses to Biochars  
603 Varying in Particle Size, Surface and Pore Properties. *Pedosphere [J]*, 25: 770-  
604 780.
- 605 Kambo H S, Dutta A 2015. A comparative review of biochar and hydrochar in terms  
606 of production, physico-chemical properties and applications. *Renewable and  
607 Sustainable Energy Reviews [J]*, 45: 359-378.
- 608 Khalid Z B, Siddique M N I, Nayeem A, et al. 2021. Biochar application as  
609 sustainable precursors for enhanced anaerobic digestion: A systematic review.  
610 *Journal of Environmental Chemical Engineering [J]*, 9: 105489.
- 611 Klupfel L, Keiluweit M, Kleber M, et al. 2014. Redox properties of plant biomass-  
612 derived black carbon (biochar). *Environ Sci Technol [J]*, 48: 5601-5611.
- 613 Koch B P, Dittmar T 2006. From mass to structure: an aromaticity index for high-  
614 resolution mass data of natural organic matter. *Rapid Communications in Mass  
615 Spectrometry [J]*, 20: 926-932.
- 616 Li B, Yang L, Wang C Q, et al. 2017a. Adsorption of Cd(II) from aqueous solutions  
617 by rape straw biochar derived from different modification processes.  
618 *Chemosphere [J]*, 175: 332-340.
- 619 Li H, Dong X, da Silva E B, et al. 2017b. Mechanisms of metal sorption by biochars:  
620 Biochar characteristics and modifications. *Chemosphere [J]*, 178: 466-478.
- 621 Li W, Cheng C, He L, et al. 2021. Effects of feedstock and pyrolysis temperature of  
622 biochar on promoting hydrogen production of ethanol-type fermentation. *Sci  
623 Total Environ [J]*, 790: 148206.
- 624 Li W, Khalid H, Zhu Z, et al. 2018. Methane production through anaerobic digestion:  
625 Participation and digestion characteristics of cellulose, hemicellulose and lignin.  
626 *Applied Energy [J]*, 226: 1219-1228.
- 627 Li Y, Liu H, Yan F, et al. 2017c. High-calorific biogas production from anaerobic

- 628 digestion of food waste using a two-phase pressurized biofilm (TPPB) system.  
629 *Bioresour Technol* [J], 224: 56-62.
- 630 Li Y, Qian J, Wang M, et al. 2022a. Enhanced performance of anaerobic two-phase  
631 reactor treating coal gasification wastewater with the assistance of zero valent  
632 iron under co-digestion conditions. *Chemical Engineering Journal* [J], 430:  
633 131996.
- 634 Li Y, Wang Z, Jiang Z, et al. 2022b. Bio-based carbon materials with multiple  
635 functional groups and graphene structure to boost methane production from  
636 ethanol anaerobic digestion. *Bioresour Technol* [J], 344: 126353.
- 637 Liew L N, Shi J, Li Y 2012. Methane production from solid-state anaerobic digestion  
638 of lignocellulosic biomass. *Biomass and Bioenergy* [J], 46: 125-132.
- 639 Lim E Y, Tian H, Chen Y, et al. 2020. Methanogenic pathway and microbial  
640 succession during start-up and stabilization of thermophilic food waste anaerobic  
641 digestion with biochar. *Bioresour Technol* [J], 314: 123751.
- 642 Lv W, Schanbacher F L, Yu Z 2010. Putting microbes to work in sequence: recent  
643 advances in temperature-phased anaerobic digestion processes. *Bioresour*  
644 *Technol* [J], 101: 9409-9414.
- 645 Ni B J, Zeng S, Wei W, et al. 2020. Impact of roxithromycin on waste activated sludge  
646 anaerobic digestion: Methane production, carbon transformation and antibiotic  
647 resistance genes. *Sci Total Environ* [J], 703: 134899.
- 648 Pan J, Ma J, Liu X, et al. 2019. Effects of different types of biochar on the anaerobic  
649 digestion of chicken manure. *Bioresour Technol* [J], 275: 258-265.
- 650 Qi Q, Sun C, Cristhian C, et al. 2021. Enhancement of methanogenic performance by  
651 gasification biochar on anaerobic digestion. *Bioresour Technol* [J], 330: 124993.
- 652 Qin Y, Yin X, Xu X, et al. 2020. Specific surface area and electron donating capacity  
653 determine biochar's role in methane production during anaerobic digestion.  
654 *Bioresour Technol* [J], 303: 122919.
- 655 Qu J, Wang Y, Tian X, et al. 2021. KOH-activated porous biochar with high specific  
656 surface area for adsorptive removal of chromium (VI) and naphthalene from  
657 water: Affecting factors, mechanisms and reusability exploration. *J Hazard Mater*  
658 [J], 401: 123292.
- 659 Quintana-Najera J, Blacker A J, Fletcher L A, et al. 2021. The effect of augmentation  
660 of biochar and hydrochar in anaerobic digestion of a model substrate. *Bioresour*  
661 *Technol* [J], 321: 124494.
- 662 Ren S, Usman M, Tsang D C W, et al. 2020. Hydrochar-Facilitated Anaerobic  
663 Digestion: Evidence for Direct Interspecies Electron Transfer Mediated through  
664 Surface Oxygen-Containing Functional Groups. *Environ Sci Technol* [J], 54:  
665 5755-5766.
- 666 Rotaru A-E, Shrestha P M, Liu F, et al. 2014. A new model for electron flow during  
667 anaerobic digestion: direct interspecies electron transfer to *Methanosaeta* for the  
668 reduction of carbon dioxide to methane. *Energy Environ. Sci.* [J], 7: 408-415.
- 669 Satchwell A J, Scown C D, Smith S J, et al. 2018. Accelerating the Deployment of



- 670 Anaerobic Digestion to Meet Zero Waste Goals. *Environ Sci Technol [J]*, 52:  
671 13663-13669.
- 672 Shen B, Liu Z, Xu H, et al. 2019. Enhancing the absorption of elemental mercury  
673 using hydrogen peroxide modified bamboo carbons. *Fuel [J]*, 235: 878-885.
- 674 Singh B, Fang Y, Cowie B C C, et al. 2014. NEXAFS and XPS characterisation of  
675 carbon functional groups of fresh and aged biochars. *Organic Geochemistry [J]*,  
676 77: 1-10.
- 677 Suliman W, Harsh J B, Abu-Lail N I, et al. 2016. Modification of biochar surface by  
678 air oxidation: Role of pyrolysis temperature. *Biomass and Bioenergy [J]*, 85: 1-  
679 11.
- 680 Świąteczak P, Cydzik-Kwiatkowska A, Rusanowska P 2017. Microbiota of anaerobic  
681 digesters in a full-scale wastewater treatment plant. *Archives of Environmental  
682 Protection [J]*, 43: 53-60.
- 683 Tan Z, Yuan S, Hong M, et al. 2020. Mechanism of negative surface charge formation  
684 on biochar and its effect on the fixation of soil Cd. *J Hazard Mater [J]*, 384:  
685 121370.
- 686 Vavilin V A, Qu X, Mazeas L, et al. 2008. Methanosarcina as the dominant  
687 aceticlastic methanogens during mesophilic anaerobic digestion of putrescible  
688 waste. *Antonie Van Leeuwenhoek [J]*, 94: 593-605.
- 689 Wan Z, Sun Y, Tsang D C W, et al. 2019. A sustainable biochar catalyst synergized  
690 with copper heteroatoms and CO<sub>2</sub> for singlet oxygenation and electron transfer  
691 routes. *Green Chemistry [J]*, 21: 4800-4814.
- 692 Wang G, Li Q, Li Y, et al. 2020. Redox-active biochar facilitates potential electron  
693 transfer between syntrophic partners to enhance anaerobic digestion under high  
694 organic loading rate. *Bioresour Technol [J]*, 298: 122524.
- 695 Wang P, Zhang J, Shao Q, et al. 2018. Physicochemical properties evolution of chars  
696 from palm kernel shell pyrolysis. *Journal of Thermal Analysis and Calorimetry  
697 [J]*, 133: 1271-1280.
- 698 Wu W, Li J, Lan T, et al. 2017. Unraveling sorption of lead in aqueous solutions by  
699 chemically modified biochar derived from coconut fiber: A microscopic and  
700 spectroscopic investigation. *Sci Total Environ [J]*, 576: 766-774.
- 701 Xu F, Li Y, Ge X, et al. 2018. Anaerobic digestion of food waste - Challenges and  
702 opportunities. *Bioresour Technol [J]*, 247: 1047-1058.
- 703 Xu Q, Liao Y, Cho E, et al. 2020. Effects of biochar addition on the anaerobic  
704 digestion of carbohydrate-rich, protein-rich, and lipid-rich substrates. *Journal of  
705 the Air & Waste Management Association [J]*, 70: 455-467.
- 706 Xu W, Long F, Zhao H, et al. 2021. Performance prediction of ZVI-based anaerobic  
707 digestion reactor using machine learning algorithms. *Waste Manag [J]*, 121: 59-  
708 66.
- 709 Yang X, Kang K, Qiu L, et al. 2020. Effects of carbonization conditions on the yield  
710 and fixed carbon content of biochar from pruned apple tree branches. *Renewable  
711 Energy [J]*, 146: 1691-1699.

- 712 Ye J, Hu A, Ren G, et al. 2018. Red mud enhances methanogenesis with the  
713 simultaneous improvement of hydrolysis-acidification and electrical  
714 conductivity. *Bioresour Technol* [J], 247: 131-137.
- 715 Yu Z, Leng X, Zhao S, et al. 2018. A review on the applications of microbial  
716 electrolysis cells in anaerobic digestion. *Bioresour Technol* [J], 255: 340-348.
- 717 Zhang P, Liu S, Tan X, et al. 2019a. Microwave-assisted chemical modification  
718 method for surface regulation of biochar and its application for estrogen removal.  
719 *Process Safety and Environmental Protection* [J], 128: 329-341.
- 720 Zhang W, Li L, Wang X, et al. 2020. Role of trace elements in anaerobic digestion of  
721 food waste: Process stability, recovery from volatile fatty acid inhibition and  
722 microbial community dynamics. *Bioresour Technol* [J], 315: 123796.
- 723 Zhang Y, Li J, Liu F, et al. 2018a. Reduction of Gibbs free energy and enhancement of  
724 Methanosaeta by bicarbonate to promote anaerobic syntrophic butyrate  
725 oxidation. *Bioresour Technol* [J], 267: 209-217.
- 726 Zhang Y, Xu X, Cao L, et al. 2018b. Characterization and quantification of electron  
727 donating capacity and its structure dependence in biochar derived from three  
728 waste biomasses. *Chemosphere* [J], 211: 1073-1081.
- 729 Zhang Z, Zhu Z, Shen B, et al. 2019b. Insights into biochar and hydrochar production  
730 and applications: A review. *Energy* [J], 171: 581-598.
- 731 Zhao W, Yang H, He S, et al. 2021. A review of biochar in anaerobic digestion to  
732 improve biogas production: Performances, mechanisms and economic  
733 assessments. *Bioresour Technol* [J], 341: 125797.
- 734



**Highlights:**

- BC900 increased the cumulative methane production of food waste by 42.07%;
- BC900 increased the maximum methane production rate of glucose by 17.80%;
- RBC600 was inferior to BC900, but superior to BC600 in anaerobic methanation;
- Electron donating capacities and electrical conductivity of biochar are keys factors;
- Higher pyrolysis temperature and lower phenolic hydroxyl of biochar are beneficial.

Journal Pre-proof

**Declaration of interests**

The authors declare that they have no known competing financial interests or personal relationships that could have appeared to influence the work reported in this paper.

The authors declare the following financial interests/personal relationships which may be considered as potential competing interests:

Journal Pre-proof